Received: 29 July 2018 | Revised: 5 December 2018 | Accepted: 9 December 2018

DOI: 10.1002/hbm.24500

WILEY

RESEARCH ARTICLE

White matter during concussion recovery: Comparing diffusion tensor imaging (DTI) and neurite orientation dispersion and density imaging (NODDI)

Nathan W. Churchill[1,2] | Eduardo Caverzasi[3] | Simon J. Graham[4,5] | Michael G. Hutchison[2,6] | Tom A. Schweizer[1,2,7]

[1]Neuroscience Research Program, St. Michael's Hospital, Toronto, Ontario, Canada

[2]Keenan Research Centre of the Li Ka Shing Knowledge Institute at St. Michael's Hospital, Toronto, Ontario, Canada

[3]Department of Neurology, University of California, San Francisco, California

[4]Physical Sciences Platform, Sunnybrook Research Institute, Toronto, Ontario, Canada

[5]Department of Medical Biophysics, University of Toronto Faculty of Medicine, Toronto, Ontario, Canada

[6]Faculty of Kinesiology and Physical Education, University of Toronto, Toronto, Ontario, Canada

[7]Faculty of Medicine (Neurosurgery), University of Toronto, Toronto, Ontario, Canada

Correspondence
Nathan W. Churchill, 209 Victoria Street, Toronto, ON M5B 1M8, Canada.
Email: nchurchill.research@gmail.com

Funding information
Canadian Institutes of Health Research, Grant/Award Number: RN294001-367456; Canadian Institute for Military and Veterans Health, Grant/Award Number: W7714-145967; Siemens Canada Ltd.

Abstract

Concussion pathophysiology in humans remains incompletely understood. Diffusion tensor imaging (DTI) has identified microstructural abnormalities in otherwise normal appearing brain tissue, using measures of fractional anisotropy (FA), axial diffusivity (AD), and radial diffusivity (RD). The results of prior DTI studies suggest that acute alterations in microstructure persist beyond medical clearance to return to play (RTP), but these measures lack specificity. To better understand the observed effects, this study combined DTI with neurite orientation dispersion and density imaging (NODDI), which employs a more sophisticated description of water diffusion in the brain. A total of 66 athletes were recruited, including 33 concussed athletes, scanned within 7 days after concussion and at RTP, along with 33 matched controls. Both univariate and multivariate methods identified DTI and NODDI parameters showing effects of concussion on white matter. Spatially extensive decreases in FA and increases in AD and RD were associated with reduced intra-neurite water volume, at both the symptomatic phase of injury and RTP, indicating that effects persist beyond medical clearance. Subsequent analyses also demonstrated that concussed athletes with higher symptom burden and a longer recovery time had greater reductions in FA and increased AD, RD, along with increased neurite dispersion. This study provides the first longitudinal evaluation of concussion from acute injury to RTP using combined DTI and NODDI, significantly enhancing our understanding of the effects of concussion on white matter microstructure.

KEYWORDS

concussion, DTI, NODDI, white matter

1 | INTRODUCTION

Concussion is a "mild" form of traumatic brain injury, in which the transmission of impulsive force to the brain leads to altered function, including disturbances in cognition, physical function, mood and sleep (McCrory et al., 2013). The clinical management of sport-related concussion is primarily based on symptom assessments and brief cognitive testing, with the determination of return to play (RTP) made when symptoms are resolved following a graded exercise protocol. Despite symptom dissipation at RTP, there is growing evidence that concussion may lead to long-term deficits, including elevated risk of cognitive and behavioral problems (Guskiewicz et al., 2005; Guskiewicz, Ross, & Marshall, 2001). These sequelae are well documented, but much remains unknown regarding the evolution of brain physiology from the symptomatic phase of injury to medical clearance, limiting the ability of neuroimaging to inform clinical practice.

Concussion is rarely associated with findings on conventional radiological imaging; however, there is mounting evidence that concussion and its sequelae are associated with subtler alterations in brain tissue (McCrea et al., 2017). In this respect, advanced magnetic resonance imaging (MRI) using diffusion tensor imaging (DTI) is a promising tool for assessing the effects of mild traumatic brain injury (TBI). Alterations in tissue microstructure may lead to significant changes in the rate and directionality of water diffusion within white

matter tracts, where fiber bundles exhibit highly restricted and anisotropic water diffusion. DTI is able to detect these changes and has been widely used in studies involving more severe TBI, as a biomarker of axonal injury and degeneration (Hulkower, Poliak, Rosenbaum, Zimmerman, & Lipton, 2013).

In recent years, diffusion-weighted imaging of concussion has become an active area of research, with a growing body of literature examining longitudinal recovery after a concussion (Cubon, Putukian, Boyer, & Dettwiler, 2011; Meier et al., 2016; Murugavel et al., 2014), along with the subtler effects of sub-concussive impacts (Bazarian, Zhu, Blyth, Borrino, & Zhong, 2012; McAllister et al., 2014). In a recent study, DTI was used to examine the white matter of concussed athletes longitudinally, from the first week post-injury to medical clearance to RTP (Churchill, Hutchison, et al., 2017b). The primary findings were decreased fractional anisotropy (FA) and increased mean diffusivity (MD) relative to uninjured controls at the early symptomatic phase of injury, which were effects that remained present at RTP. However, standard DTI metrics are based on a simplistic model of brain tissue microstructure, consisting of a single water compartment with anisotropic Gaussian diffusion of water molecules. Thus, traditional DTI measures lack specificity, with differences in FA and diffusivity potentially arising from multiple mechanisms, including changes in cell morphology and packing density, along with alterations in white matter fiber orientation. The interpretation of differences in FA and diffusivity may also be confounded by changes in the partial volume contribution of free water from cerebrospinal fluid (CSF).

The present study addressed these limitations by applying the diffusion MRI model known as neurite orientation dispersion and density imaging (NODDI) (Zhang, Schneider, Wheeler-Kingshott, & Alexander, 2012). This method acquires data for multiple different diffusion weightings, with each acquisition sampling many different spatial orientations at a high angular resolution. These data, along with a three-compartment model of diffusion, are used to estimate the water contributions of different tissue types within each voxel. The NODDI model also calculates the orientation dispersion index (ODI), which quantifies angular deviation between neurites, which can more accurately assess neurite dispersion than FA, particularly in areas of complex neurite geometry (e.g., fanning or crossing fibers). The NODDI model shows promise as a tool for investigating concussion, with evidence that it is sensitive to the effects of repeated head impacts (Mayer et al., 2017). More recently, NODDI was used to characterize the long-term effects of concussion (Churchill, Caverzasi, Graham, Hutchison, & Schweizer, 2017a), showing that a history of concussion is associated with elevated FA and decreased MD, along with concurrent increases in neurite water volume and decreases in ODI.

The principal aim of this study was to determine whether alterations in DTI measures of FA and diffusivity among concussed athletes, seen at the early symptomatic phase of injury and RTP, are associated with concurrent changes in advanced NODDI measures. An important secondary aim was to determine whether individual variations of diffusion parameters within the concussed group were associated with clinical covariates of interest. Researchers have investigated the relationship between symptom burden and DTI parameters, but have largely focused on persistent post-concussive symptoms (Dean, Sato, Vieira, McNamara, & Sterr, 2015; Messé et al., 2013; Smits et al., 2011). To date, there has been limited investigation of the relationship between acute symptom burden and diffusion imaging parameters. Similarly, a meta-analysis of DTI and mild TBI reported significant effects of time post-injury (Eierud et al., 2014), but the relationship between diffusion imaging and time to RTP remains under-studied. Therefore, the present study examined the relationship between diffusion imaging parameters and clinical covariates, including time to RTP and acute symptom severity. Analyses were performed using both nonparametric univariate methods and a multivariate approach, termed N-way partial least squares (NPLS) (Bro, 1996), which identifies simultaneous changes in distributed brain areas across multiple imaging parameters.

2 | METHODS

2.1 | Study participants

A total of 66 athletes were recruited from seven university teams (volleyball, hockey, soccer, football, rugby, basketball, and lacrosse) at a single institution, via the university sport medicine clinic. This included 33 concussed athletes and 33 controls, individually matched to concussed athletes on age, sex and prior concussion history. For concussed athletes, diagnosis was determined by staff physician following events where athletes sustained direct or indirect contact to the head with the presence of signs and/or symptoms. The concussed athletes were scanned at two time-points: the early symptomatic phase of injury (1–7 days post-concussion) and following medical clearance to return to play (RTP). From the initial design, 2 athletes could not be scanned at symptomatic injury (N = 31 remaining) and 5 athletes had missing RTP data (N = 27 remaining). All athletes were recruited and imaged at the start of their respective seasons, and had pre-season assessments with the Sport Concussion Assessment Tool 3 (SCAT3) (Guskiewicz et al., 2013) to evaluate symptoms, cognition and balance, ensuring that there were no significant deficits in controls or in concussed athletes prior to their injury. The study procedures were approved by institutional review boards at the University of Toronto and St. Michael's Hospital in Toronto, and all athletes gave written informed consent prior to study participation.

2.2 | Magnetic resonance imaging

Participants were imaged at St. Michael's Hospital using an MRI system operating at 3 Tesla (Magnetom Skyra, Siemens, Erlangen, Germany) with the standard multi-channel head receiver coil. To assess for structural lesions, 3D T1-weighted Magnetization Prepared Rapid Acquisition Gradient Echo (MPRAGE) images were acquired with field-of-view (FOV) = 24 × 24cm, 240 × 240 × 192 acquisition matrix, 0.9 mm isotropic voxels, bandwidth = 250 Hz/Pixel, inversion time (TI)/echo time (TE)/repetition time (TR) = 850/2.63/2,000 ms, and flip angle (FA) = 8°. Fluid attenuated inversion recovery imaging (FLAIR) was also obtained with FOV = 22 × 18.6 cm, 256 × 196 acquisition matrix, 1.1 × 0.9 × 3.0 mm voxels, TI/TE/TR = 2,200/96/9,000 ms. To assess for potential vascular abnormalities, susceptibility-weighted imaging (SWI) was also performed with FOV = 22 × 19.2 cm, 0.6 ×

0.6 × 1.2 mm voxels with an encoding gap of 0.2 mm, TR/TE = 28/20 ms, FA = 15°, and 384 × 307 acquisition matrix. Structural scans were first reviewed by an MRI technologist; if abnormalities were identified, they were then reviewed by a neuroradiologist and reported. Statistical outlier testing was also performed to further check for structural abnormalities: from the control group, global statistics were calculated on the masked brain images (mean, variance, skew, and kurtosis) of T1, FLAIR, and SWI scans. For each statistic and scan type, a gamma distribution was fit to the control data and subsequent testing identified any athletes, control or concussed, that were outliers at $p < 0.05$ (Bonferroni-adjusted). No athletes showed evidence of structural abnormalities, based on visual inspection or statistical analysis.

A two-shell protocol was used for diffusion MRI, to enable standard estimation of single-shell DTI parameters as well as the multi-shell NODDI parameters (FOV = 24 × 24 cm, 120 × 120 acquisition matrix, 66 slices, 2 × 2 × 2 mm voxels, bandwidth 1,736 Hz/Px). The first acquisition consisted of 30 diffusion-weighting directions at TR/TE = 7,800/83 ms and b = 700 s/mm^2, along with 9 b0 scans. The second acquisition consisted of 64 diffusion-weighting directions at TR/TE = 12,300/91 ms and b = 2,000 s/mm^2, along with 1 b0 scan.

2.3 | Preprocessing

For diffusion-weighted MRI data, the FMRIB Software Library (FSL; www.fmrib.ox.ac.uk/fsl) was used to perform simultaneous correction of eddy current distortions and rigid-body head motion using the FSL *eddy* protocol, and nonbrain voxels were masked out by applying FSL *bet* to the subject b0 images. The data were then analyzed to extract voxel-wise DTI metrics including fractional anisotropy (FA), axial diffusivity (AD), and radial diffusivity (RD) using FSL *dtifit*. The diffusivity components were analyzed instead of mean diffusivity (MD), as they provide a more detailed representation of water diffusion; in multivariate analysis MD is also redundant, as it can be represented as a linear combination of AD and RD. The results presented in this article are based on the b = 700, 30-direction shell, thereby avoiding signal attenuation and restricted diffusion effects in the b = 2,000, 64-direction shell acquired at the higher b-value. Univariate analyses of the DTI parameters derived from the 64-direction data found no significant effects of concussion and are therefore not further discussed in this article.

Because the two diffusion imaging shells had different TR/TE values, they were normalized prior to NODDI analyses by dividing diffusion-weighted voxel values by the corresponding voxel value of the initial b0 scan in each shell, an approach that has been previous applied (Chang et al., 2015; Churchill, Caverzasi, et al., 2017a; Owen et al., 2014). As part of this study, simulations were performed demonstrating that this correction strategy may mitigate the fitting error induced by mismatched TR/TE between shells (Supporting Information Appendix S1). The NODDI analyses were conducted on the normalized data using the Matlab toolbox (nitrc.org/projects/noddi_toolbox) with a "WatsonSHStickTortIsoV_B0" model parameterization and default values of neural diffusivity (1.7 μm/ms) and isotropic diffusivity (3.0 μm/ms).

In the NODDI model, tissue water within each voxel is partitioned into three volume fractions: free water contributed by CSF, having isotropic Gaussian diffusion (V_{ISO}); intracellular water in neurites, having anisotropic restricted diffusion (V_{IC}); and extracellular water, having anisotropic hindered diffusion (V_{EC}). Since total volume fraction sums to unity, this is expressed as:

$$V_{ISO} + (1 - V_{ISO})(V_{IC} + V_{EC}) = 1$$

For which the anisotropic compartments also sum to unity, i.e., $V_{EC} + V_{IC} = 1$. The intracellular signal is modeled as a Watson distribution over cylinders of zero radius, with a mean orientation parameter μ and a concentration parameter $\kappa \in (0, \infty)$ indicating sharpness of the distribution around μ. The concentration parameter is transformed into the orientation dispersion index, $ODI = (2/\pi)\arctan(\kappa)$, which is a bounded value ranging from 0 (completely parallel neurites) to 1 (completely random neurite orientation). Because of unknown, potentially complex evolving brain pathophysiology, this study examined multiple DTI parameters (FA, AD, RD) and NODDI parameters (ODI, V_{ISO}, V_{IC}), with V_{EC} excluded because of its reciprocal relationship with V_{IC}.

To enable comparisons of the diffusion MRI parameters between athletes, data were co-registered to a common group-specific template, using the DTI-TK software package (dti-tk.sourceforge.net), which shows robust performance when aligning diffusion-weighted data by aligning directly on the tensor (Wang et al., 2011). To avoid subject bias in this longitudinal design, the initial template was constructed using each control subject, and one timepoint (symptomatic injury or RTP) from each concussed athlete. The timepoint was randomly selected per athlete, to also avoid biasing the template fit toward a specific time post-injury. Template bootstrapping was conducted using the IXI Aging DTI Template 3.0 (www.nitrc.org/frs/download.php/5518/ixi_aging_template_v3.0.tgz). A stepwise procedure was then conducted: (1) a bootstrapped template was estimated using *dti_template_bootstrap*; (2) tensor data were aligned affinely to update the bootstrap template using *dti_affine_population* with the Euclidean distance squared (EDS) similarity metric and three iterations; this was followed by diffeomorphic alignment using *dti_diffeomorphic_population* with ftol = 0.002 and six iterations. For the remaining concussed athlete maps, transforms to the pre-defined group template were obtained by sequentially applying *dti_rigid_sn* and *dti_affine_sn* with the EDS metric, followed by *dti_diffeomorphic_sn* with six iterations and ftol = 0.002. The net transforms for all datasets were then computed using *dfRightComposeAffine* and applied to DTI and NODDI parameter maps via *deformationScalarVolume* with resampled voxel dimensions of 2 × 2 × 2 mm isotropic.

For DTI and NODDI parameter maps, a mask of voxels with mean FA ≥ 0.30 was constructed to restrict analyses to white matter tracts. To reduce the impact of fine-grained local variation in anatomy between individuals, voxels within the mask region were then convolved with a 6 mm FWHM 3D Gaussian smoothing kernel. Regions outside the mask were given zero weights during convolution, to reduce confounds due to nonwhite matter tissue. In addition, the brainstem and cerebellum were manually segmented and removed before analysis, to avoid confounds due to substantial magnetic field inhomogeneity in these regions.

2.4 | Analyses

2.4.1 | Univariate analysis

For each DTI and NODDI parameter, analysis was performed on (1) the voxel-wise mean difference between symptomatic concussed athletes (SYM) and controls (CTL), along with (2) the voxel-wise mean longitudinal change from SYM to RTP. Significance was evaluated nonparametrically by bootstrapping the mean in a repeated-measures design (1,000 iterations), where resampling units consisted of a SYM athlete scan and their matched CTL or RTP scan. Voxels were then identified where the bootstrapped 95% confidence intervals (CIs) did not include zero effect, after adjusting for multiple comparisons. This was done by retaining all voxels where the 99.5% CI did not include zero (p = 0.005 two-tailed significance), then cluster-size thresholding at p = 0.05 using the Analysis of Functional NeuroImages (AFNI) *3dFWHMx* function to estimate spatial smoothness, followed by AFNI *3dClustSim* to estimate the corresponding minimum cluster-size threshold. For significant brain voxels, effect size was reported as the bootstrap ratio (bootstrapped mean/standard error). Post-hoc testing was also done to evaluate between-group differences in diffusion parameters, averaged over significant brain regions, including the mean and 95%CI, along with p-values based on nonparametric paired-measures Wilcoxon tests.

2.4.2 | Multivariate analysis

The data were also examined using a multivariate approach termed N-way Partial Least Squares (NPLS) (Bro, 1996). This is an extension of standard PLS (Krishnan, Williams, McIntosh, & Abdi, 2011), which identifies latent covariance relationships between brain imaging and behavioral data. Whereas PLS quantifies two-way relationships (e.g., between voxel values and behavior, for a single diffusion parameter), NPLS accounts for higher-order relationships in input data (e.g., between voxel values and behavior, over multiple diffusion parameters). This model was used to test for white matter regions showing simultaneous effects of concussion for the 6 DTI/NODDI parameters. The approach has greater sensitivity than univariate methods, as NPLS can detect distributed patterns in the brain and leverage shared information across diffusion parameters. As a latent variable model, it is also robust to high-dimensional, highly-correlated data (Churchill et al., 2013), where standard regression methods may be ill-posed and require careful regularization for a stable solution. The NPLS model is described below.

In neuroimaging PLS, two multivariate datasets are analyzed for subjects s = 1…S, including a ($V \times 1$) vector of voxel values $\boldsymbol{x}_s$ (e.g., a diffusion parameter map) and a ($B \times 1$) vector of behavioral values $\boldsymbol{y}_s$ (e.g., condition labels or clinical variables). The model quantifies shared information between $\boldsymbol{x}$ and $\boldsymbol{y}$, by decomposing the data into k = 1…K pairs of latent variables (c_k^x, c_k^y) that have greatest covariance. For the kth latent variable pair, the PLS model seeks weighting vectors $\boldsymbol{w}_k^x$ and $\boldsymbol{w}_k^y$ that produce latent variables $c_{k(s)}^x = \boldsymbol{x}_s{}^T \boldsymbol{w}_k^x$ and $c_{k(s)}^y = \boldsymbol{y}_s{}^T \boldsymbol{w}_k^y$, which maximize the covariance:

$$cov(c_k^x, c_k^y) = cov\left(\boldsymbol{w}_k^{x\,T}\boldsymbol{x}_s, \boldsymbol{w}_k^{y\,T}\boldsymbol{y}_s\right), \quad \text{such that} \quad \|\boldsymbol{w}_k^x\| = \|\boldsymbol{w}_k^y\| = 1.$$

usually under the constraint that $\{\boldsymbol{w}_k^x, \boldsymbol{w}_k^y\}$ are orthogonal to the preceding $k-1$ weighting vectors.

This approach may be extended to input data with higher-order structure using NPLS (Bro, 1996), as in the case where m = 1…M different brain maps have been acquired (e.g., diffusion parameter maps). This can be expressed as a ($V \times M$) matrix $\boldsymbol{X}_s$ for each subject. The NPLS model now seeks weighting vectors $\boldsymbol{w}_{k(1)}^x$, $\boldsymbol{w}_{k(2)}^x$, and $\boldsymbol{w}_k^y$, producing latent variables $c_{k(s)}^x = \boldsymbol{w}_{k(1)}^{x\,T}\boldsymbol{X}_s\boldsymbol{w}_{k(2)}^x$ and $c_{k(s)}^y = \boldsymbol{y}_s{}^T\boldsymbol{w}_k^y$, which maximize the covariance:

$$cov(c_k^x, c_k^y) = cov\left(\boldsymbol{w}_{k(1)}^{x\,T}\boldsymbol{X}_s\boldsymbol{w}_{k(2)}^x, \boldsymbol{y}_s{}^T\boldsymbol{w}_k^y\right), \quad \text{such that} \quad \left\|\boldsymbol{w}_{k(1)}^x\right\| = \left\|\boldsymbol{w}_{k(2)}^x\right\| = \|\boldsymbol{w}_k^y\| = 1$$

These components are estimated using an iterative update algorithm (Bro, 1996), producing k = 1…K orthogonal component sets $\left\{\boldsymbol{w}_{k(1)}^x, \boldsymbol{w}_{k(2)}^x, \boldsymbol{w}_k^y\right\}$, where for high-dimensional neuroimaging data, the maximum number of components is generally $K \leq rank(\boldsymbol{Y})$.

For the main analysis of this study, the input data matrix $\boldsymbol{X}_s$ consisted of the six diffusion parameter maps, and the response variable $\boldsymbol{y}_n$ was the set of binary labels denoting membership to CTL, SYM, or RTP groups. Thus, for a CTL scan $\boldsymbol{y}_n$ = [1 0 0], for a SYM scan $\boldsymbol{y}_n$ = [0 1 0] and for an RTP scan $\boldsymbol{y}_n$ = [0 0 1]. The NPLS "voxel saliences" $\boldsymbol{w}_{k(1)}^x$ and "diffusion parameter saliences" $\boldsymbol{w}_{k(2)}^x$ reflect the combination of brain regions and DTI/NODDI parameters that have maximal covariation between athlete groups, with group weightings given by "behavioral saliences" $\boldsymbol{w}_k^y$. The reliability of the saliences was assessed via bootstrapping on subjects (1,000 iterations). The significant voxel saliences were then identified at an adjusted p = 0.05 using the cluster-size correction procedure described for univariate methods above. The diffusion parameter and behavioral variable saliences were also identified for cases where the bootstrapped 95% CIs did not include zero. These values were corrected for multiple comparisons at a False-Discovery Rate (FDR) of 0.05. To be considered valid, a component was required to have significant saliences for voxels, diffusion parameters and behavior. The "brain scores" c_k^x were also plotted as a function of athlete group and the mean between-group differences and 95%CI reported, with significant group differences reported when bootstrapped 95% CIs did not include zero after FDR adjustment.

A secondary analysis was conducted within the concussed cohort, to test whether the longitudinal evolution of diffusion imaging measures from SYM to RTP is affected by clinical covariates. For this analysis, the input data matrix was the pairwise change from SYM to RTP $\boldsymbol{X}_n^{'} = \boldsymbol{X}_n^{(RTP)} - \boldsymbol{X}_n^{(SYM)}$ and the response variables were two clinical measures: (1) symptom severity and (2) days to RTP. Symptoms were assessed based on the SCAT3 total severity score, which was obtained by summing across a 22-item symptom scale, each with a 7-point Likert scale rating (Guskiewicz et al., 2013). Days to RTP was determined as the number of days from the concussion event to complete symptom resolution, following a graded exertional protocol (McCrory et al., 2017). To ensure robust covariance estimates, rank-normalization was applied to both symptom severity (kurtosis = 4.27, significantly non-normal at p = 0.039) and days to RTP (kurtosis = 4.87, p = 0.016), as heavy distribution tails in behavioral data may lead to unstable bootstrap estimates. The MRI data were not transformed, as rank-normalization showed no significant effect on NPLS saliences. This was expected, as all diffusion parameters had a median

kurtosis ≤3.47 (p = 0.139). As in the previous section, significant voxel, diffusion parameter and behavioral saliences were identified after adjusting for multiple comparisons.

3 | RESULTS

3.1 | Participant demographics

The athlete demographics and clinical data are summarized in Table 1, for control and concussed athlete groups. For concussed athletes, the median time to RTP was 19 days (interquartile range: 13–58) and ranged from a minimum of 4 days to a maximum of 236 days. At the initial symptomatic timepoint, concussed athletes had significantly elevated total symptoms and symptom severity compared with their pre-season baseline (median and interquartile range, symptoms: 5, [2, 11], p = 0.006; severity: 7, [2, 27], p = 0.012, paired-measures Wilcoxon tests), and relative to the matched control athletes (symptoms: 5, [1, 12], p = 0.001; severity: 6, [0, 31]; p = 0.004). All effects were significant at an FDR of 0.05. At RTP, total symptoms and symptom severity were no longer significantly increased relative to baseline or controls ($p \geq 0.45$ for all tests). Balance and cognition scores were not significantly different between symptomatic injury and baseline, nor were they different from matched controls ($p \geq 0.361$ for all tests).

3.2 | Univariate analysis

Figure 1 depicts the results of univariate analysis. The top row shows the mean unsmoothed brain map for each parameter, calculated voxel-wise across all control subjects. The second row depicts areas of significant difference for concussed athletes at SYM relative to CTL (see Table 2 for clusters and Table 3 for group comparison statistics). Sparse decreases in FA were seen within the corpus callosum, while elevated AD was observed within the corona radiata. More spatially extensive areas of increased RD were also observed, including the corona radiata, corpus callosum, and external capsule. In contrast, among the NODDI parameters only V_{IC} showed significant effects at SYM, including decreases within the corona radiata and longitudinal fasciculus. For all identified brain regions, the differences relative to CTL were significant at SYM and remained significant at RTP, but there was no evidence of significant longitudinal change.

The third row depicts areas of longitudinal change from SYM to RTP (see Table 2 for clusters and Table 4 for group comparison statistics). Decreased FA was seen in the internal capsule, corpus callosum and corona radiata, along with reduced AD near the external capsule. Effects on RD were more spatially complex, including increases in the splenium of the corpus callosum and posterior thalamic radiation, but also decreases in the body of the corpus callosum and internal capsule. For the NODDI parameters, only ODI showed a significant longitudinal increase over time, near the uncinate fasciculus. While these diffusion parameters had significant longitudinal effects, the identified areas were not significantly different from CTL at SYM or RTP, after adjusting for multiple comparisons.

3.3 | Multivariate analysis

Results of the NPLS analysis of concussion effects are depicted in Figure 2, where only a single component was identified after adjusting for multiple comparisons (68.9% of NPLS covariance), with clusters reported in Table 5. For this component, a widespread set of white matter regions showed significant concussion effects (Figure 2a), with two bilateral clusters centered on the superior corona radiata and a smaller cluster near the posterior thalamic radiation. Within these regions, decreased FA was observed concurrently with increased diffusivity for both AD and RD, along with decreased V_{IC} (Figure 2b), whereas ODI and V_{ISO} effects were non-significant. As depicted in Figure 1c, the mean response was significantly elevated in concussed athletes relative to the CTL group, at both SYM (mean difference and 95%CI: 0.659 [0.213, 1.07]; p = 0.008) and RTP (mean difference and 95%CI: 0.738 [0.294,

TABLE 1 Demographic data for athletes with concussion and matched controls, along with symptom and cognitive scores, based on the sport concussion assessment tool (SCAT3)

	Control		Concussion	
Age (mean ± *SD*)	20.5 ± 1.7		20.3 ± 2.0	
Female	17/33 (52%)		17/33 (52%)	
Previous concussion	19/33 (58%)		19/33 (58%)	
Days to RTP	–		19 [13, 58]	
		Baseline	SYM	RTP
Total symptoms	2 [0, 5]	2 [0, 5]	8 [4, 15]**	0 [0, 2]
Symptom severity	2 [0, 5]	2 [0, 7]	9 [4, 31]**	0 [0, 2]
Orientation	5 [5, 5]	5 [5, 5]	5 [5, 5]	5 [5, 5]
Immediate memory	15 [14,15]	14 [14, 15]	15 [14, 15]	15 [15, 15]
Concentration	4 [3, 4]	3 [2, 4]	4 [3, 5]	4 [3, 4]
Delayed memory	4 [4, 5]	4 [3, 5]	4 [3, 5]	5 [4, 5]
Balance Total errors	2 [1, 3]	3 [0, 4]	3 [1, 5]	1 [0, 2]

The SCAT3 scores are represented as the median [Q1, Q3]. "**" indicates a significant difference in scores for the symptomatic time-point (SYM), relative to all other groups. Only Total symptoms and symptom severity were significantly elevated at SYM, relative to baseline and matched controls.

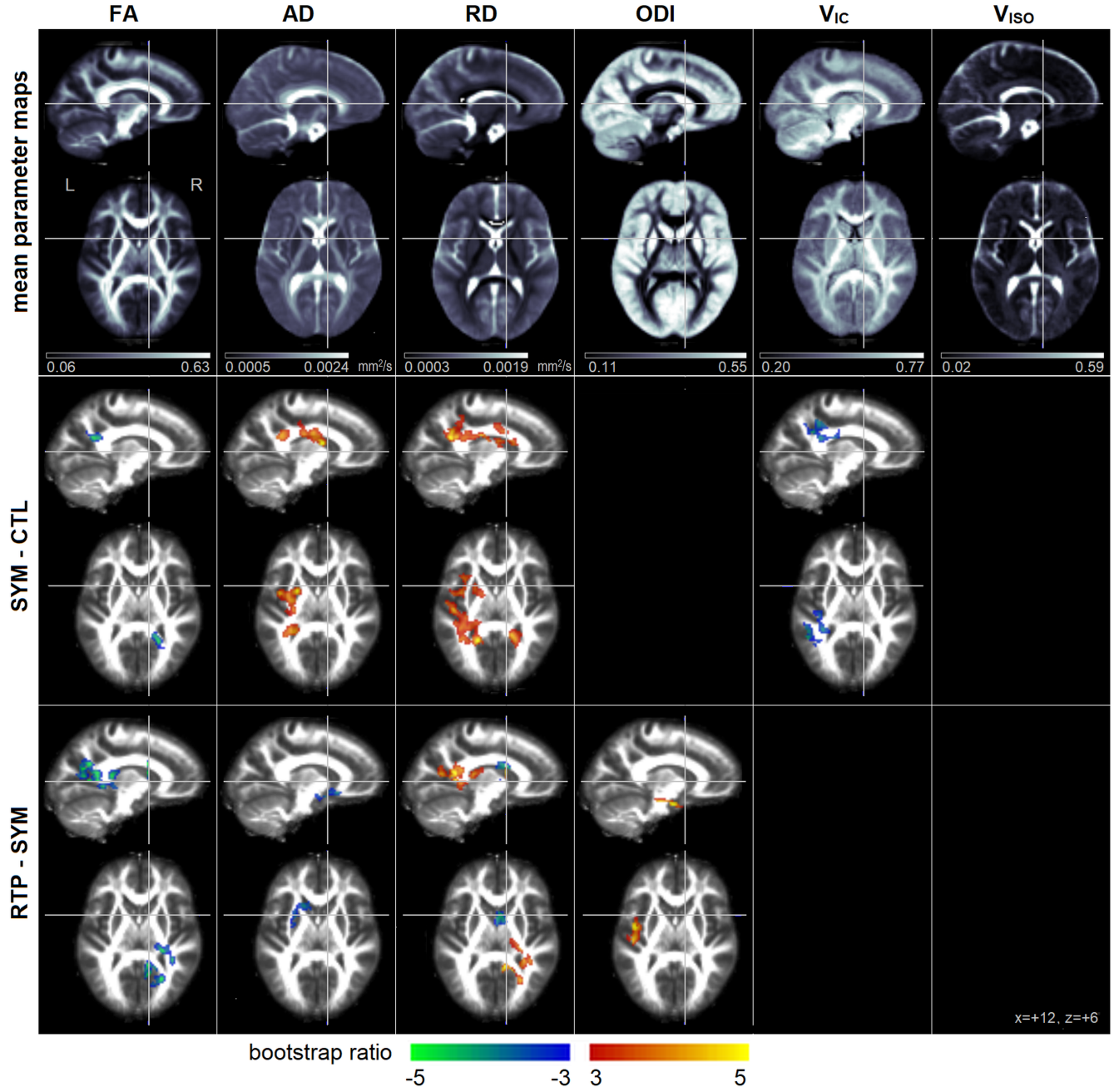

FIGURE 1 (Top row) Mean voxel-wise DTI and NODDI diffusion parameter maps, averaged over the control group (CTL). The DTI parameters include fractional anisotropy (FA), axial diffusivity (AD) and radial diffusivity (RD). The NODDI parameters include the orientation dispersion index (ODI), along with both intracellular water (V_{IC}) and isotropic free water (V_{ISO}) volume fractions. (Middle row) Plots depicting significant univariate group differences comparing symptomatic concussed athletes (SYM) to CTL. (Bottom row) Plots depicting significant univariate group differences comparing SYM to concussed athletes medically cleared to return to play (RTP). Effects sizes are reported as bootstrap ratios, with cluster size correction at $p = 0.05$. Results of group comparisons are shown as maximum intensity projections (MIPs) in sagittal and axial planes, centered on MNI coordinates ($x = +12$, $z = +6$) [Color figure can be viewed at wileyonlinelibrary.com]

1.15]; $p = 0.002$), although only 3 SYM scans and 2 RTP scans exceeded the normal 95% CIs of the CTL group (i.e., the horizontal dashed lines). Although the median brain score was higher at RTP than SYM, longitudinal changes were nonsignificant (mean change and 95%CI: 0.037 [−0.137, 0.200]; $p = 0.66$).

For the NPLS covariate analysis of the change in diffusion imaging from SYM to RTP, only a single significant component was found after adjusting for multiple comparisons (63.3% of NPLS covariance). For this component, brain areas showing significant covariate effects (Figure 3a) were spatially limited to a single cluster, reported in Table 5, which was centered on the superior longitudinal fasciculus. Within this cluster, concurrent longitudinal decreases in FA and increases in AD and RD were observed, along with increased ODI (Figure 3b), whereas V_{IC} and V_{ISO} showed nonsignificant effects. The diffusion imaging effects were associated with elevated acute symptom severity and longer time to RTP among concussed athletes (Figure 3c). As shown by the plot of brain and behavior scores (Figure 3d) these effects had a strong multivariate association (correlation and 95%CI: 0.758, [0.578, 0.890]; $p < 0.001$).

TABLE 2 Cluster report for univariate analysis of diffusion parameters in Figure 1

		Cluster	Center of mass			Brain region	Cluster size (mm^3)	Peak value (bootstrap ratio)
SYM - CTL	FA	1	21	−51	22	Corpus callosum, splenium R	664	−4.71
	AD	1	−27	−5	22	Superior corona radiata	2,408	5.52
		2	−29	−41	22	Posterior corona radiata L	1,000	4.14
	RD	1	−29	−39	24	Posterior corona radiata L	3,416	5.14
		2	17	−45	26	Corpus callosum, splenium R	1,120	4.35
		3	−29	7	16	External capsule L	656	3.80
		4	−21	1	30	Superior corona radiata L	616	3.55
	ODI	n/a						
	V_{IC}	1	−39	−35	32	Superior longitudinal fasciculus L	856	−4.19
		2	−29	−31	22	Posterior corona radiata L	736	−3.95
	V_{ISO}	n/a						
SYM - RTP	FA	1	25	−31	14	Internal capsule, retrolent. Part R	920	−4.74
		2	15	−49	26	Corpus callosum, splenium R	832	−4.90
		3	27	−59	20	Posterior corona radiata R	696	−4.93
	AD	1	−23	15	−8	External capsule L	600	−3.98
	RD	1	17	−51	14	Corpus callosum, splenium R	912	5.37
		2	31	−41	12	Posterior thalamic radiation R	680	4.15
		3	5	5	22	Corpus callosum, body R	624	−4.44
		4	21	−23	14	Internal capsule, posterior limb R	536	4.04
	ODI	1	−39	−1	−18	Uncinate fasciculus L	624	5.27
	V_{IC}	n/a						
	V_{ISO}	n/a						

Clusters are identified, with centers of mass in MNI coordinates and brain region based on nearest labeled white matter tract in the Johns Hopkins University (JHU) atlas. Peak values are reported as the highest bootstrap ratio within each cluster.

TABLE 3 Analysis of diffusion parameter values for brain areas identified in univariate between-group analysis of symptomatic concussed athletes (SYM) relative to controls (CTL) in Figure 1 (middle row)

	SYM-CTL	*p*	RTP-CTL	*p*	RTP-SYM	*p*
FA ($\times 10^{-2}$)	−2.07 [−3.00, −1.19]	<0.001	−2.39 [−3.27, −1.41]	<0.001	−0.29 [−0.65, 0.05]	0.202
AD mm^2/s ($\times 10^{-5}$)	2.89 [1.93, 3.88]	<0.001	2.48 [1.44, 3.56]	<0.001	0.03 [−0.88, 0.24]	0.301
RD mm^2/s ($\times 10^{-5}$)	2.45 [1.55, 3.39]	<0.001	2.40 [1.32, 3.49]	0.001	0.01 [−0.41, 0.30]	0.738
ODI	n/a					
V_{IC} ($\times 10^{-2}$)	−2.55 [−3.69, −1.42]	<0.001	−2.41 [−3.73, −1.20]	0.001	−0.10 [−0.89, 0.77]	0.605
V_{ISO}	n/a					

Pairwise comparisons are conducted between CTL, SYM, and concussed athletes at medical clearance to return to play (RTP). Results are reported as mean and repeated-measures bootstrapped 95% confidence interval, along with empirical *p*-values. Diffusivity values AD and RD are reported in units of mm^2/s, while all other measures are dimensionless and range from 0 to 1.

TABLE 4 Analysis of diffusion parameter values for brain areas identified in univariate between-group analysis of concussed athletes at medical clearance to return to play (RTP) relative to when they were symptomatic (SYM) in Figure 1 (bottom row)

	SYM-CTL	*p*	RTP-CTL	*p*	RTP-SYM	*p*
FA ($\times 10^{-2}$)	0.22 [−0.36, 0.84]	0.673	−0.81 [−1.56, 0.01]	0.041	−0.90 [−1.18, −0.62]	<0.001
AD mm^2/s ($\times 10^{-5}$)	1.13 [0.13, 2.17]	0.039	−0.10 [−1.13, 0.99]	0.923	−1.53 [−2.16, −0.92]	<0.001
RD mm^2/s ($\times 10^{-5}$)	1.05 [−0.93, 3.15]	0.290	−1.52 [−0.91, 3.97]	0.259	0.49 [−0.10, 1.16]	0.136
ODI ($\times 10^{-2}$)	0.37 [−1.82, 2.57]	0.586	3.24 [0.97, 5.55]	0.013	2.48 [1.55, 3.51]	0.001
V_{IC}	n/a					
V_{ISO}	n/a					

Pairwise comparisons are conducted between controls (CTL), SYM, and RTP. Results are reported as mean and repeated-measures bootstrapped 95% confidence interval, along with empirical *p*-values. Diffusivity values AD and RD are reported in units of mm^2/s, while all other measures are dimensionless and range from 0 to 1.

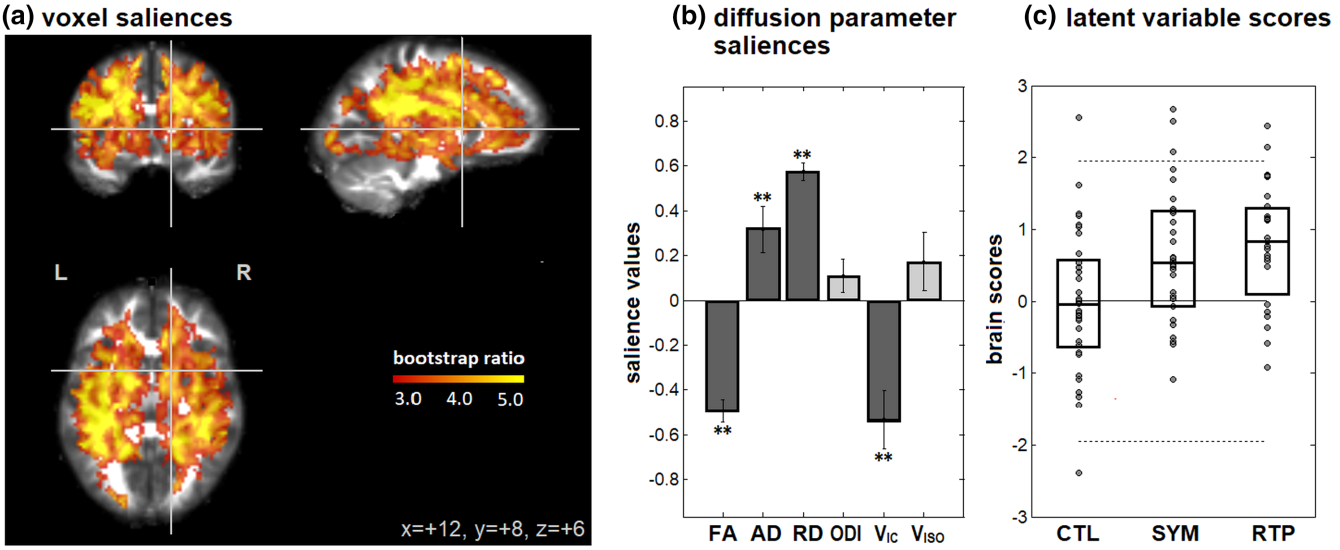

FIGURE 2 Brain regions and diffusion parameters that distinguish between athlete groups, including uninjured controls (CTL) and concussed athletes while symptomatic (SYM) and at medical clearance to return to play (RTP), based on multivariate NPLS analysis. For the single significant component, we report (a) regions with significant voxel saliences. (b) Diffusion parameter saliences that distinguish between groups in these brain regions, with error bars denoting bootstrap standard error. Significant saliences are denoted by "**." (c) Brain scores, indicating how much each subject expresses this salience pattern, along with distribution quartiles for each athlete group. The solid horizontal line = mean of CTL group scores, along with 95% confidence bounds (dashed lines), for evaluation of individual datapoints. The brain map is shown as maximum intensity projections (MIPs) in sagittal, coronal and axial planes, centered on MNI coordinates (x = +12, y = +8, z = +6) [Color figure can be viewed at wileyonlinelibrary.com]

TABLE 5 Cluster report for NPLS between-group analysis (Figure 2) and covariate analysis (Figure 3)

	Cluster	Center of Mass			Brain region	Cluster size (mm^3)	Peak value (bootstrap ratio)
Between-group analysis	1	−27	−15	22	Superior corona radiata L	49,168	9.26
	2	27	−15	23	Superior corona radiata R	44,608	9.16
	3	−23	−77	0	Posterior thalamic radiation L	872	6.35
Covariate analysis	1	31	−27	28	Superior longitudinal fasciculus R	1,608	4.10

Thirteen clusters are identified, with centers of mass in MNI coordinates and brain region based on nearest labeled white matter tract in the Johns Hopkins University (JHU) atlas. Peak values are reported as the highest bootstrap ratio within the cluster.

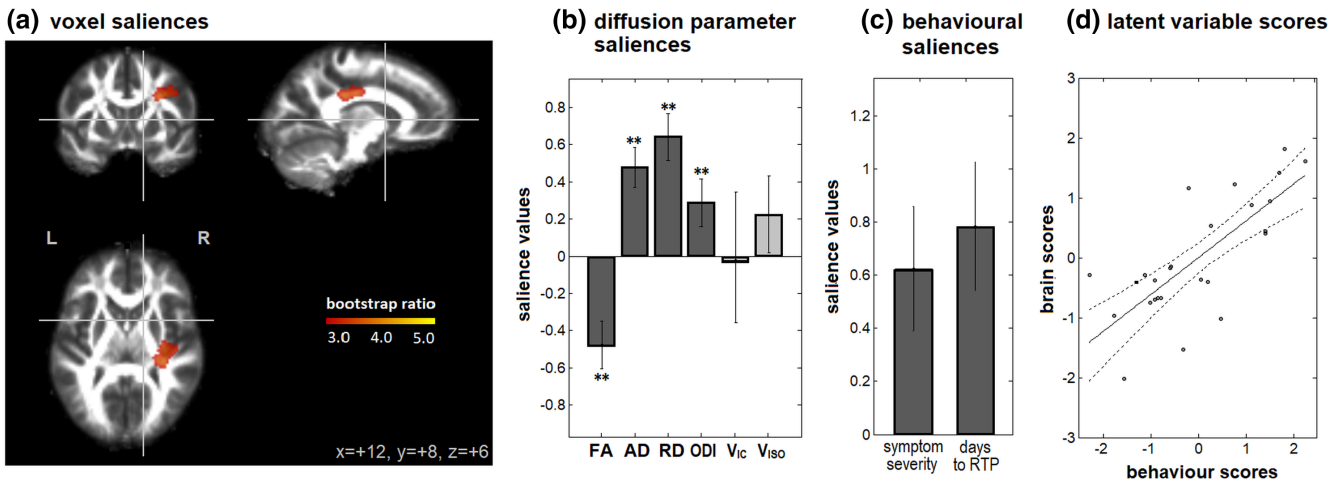

FIGURE 3 Brain regions and diffusion parameters where the longitudinal change in values is associated with clinical covariates, of SCAT symptom severity and time to RTP, based on multivariate NPLS analysis. For the single significant component, we report (a) regions with significant voxel saliences. (b) Diffusion parameter saliences that show significant covariate effects, with error bars denoting bootstrap standard error. (c) Behavioral saliences, indicating how much each covariate contributes to the relationship. Significant saliences are denoted by "**." (d) Brain and behavior scores, indicating how much each subject expresses these salience patterns. The solid line = linear regression fit, along with 95% confidence bounds (dashed lines), for evaluation of individual datapoints. The brain map is shown as maximum intensity projections (MIPs) in sagittal, coronal and axial planes, centered on MNI coordinates (x = +12, y = +8, z = +6) [Color figure can be viewed at wileyonlinelibrary.com]

4 | DISCUSSION

This study represents, to our knowledge, the first use of NODDI in the longitudinal evaluation of concussion, from the early symptomatic phase of injury to RTP. The neurobiological response to concussion is complex, and its relationship with the course of clinical recovery remains incompletely understood. This study employed both univariate voxel-wise analysis and multivariate NPLS modeling, the latter of which identified concurrent variations in DTI and NODDI parameters. The analyses showed complementary results, which affirm that the main findings are not model-dependent. In these analyses, the NODDI data were used to disentangle mechanisms of altered FA, AD, and RD, which may be influenced by changes in intra/extra-neurite water volume, altered neurite geometry, and partial volume contributions from CSF.

The current results show reduced FA with increased AD and RD at the early symptomatic phase of injury, the effects of which remain present at RTP. In addition, RD shows more spatially extensive univariate effects than AD, and has greater effect sizes for NPLS saliences, indicating that this diffusion component is a greater contributor to the observed effects. Overall, the results indicate less restricted, more isotropic water diffusion within white matter tracts, which is consistent with prior findings for a subset of these athletes (Churchill, Hutchison, et al., 2017b), along with other studies of sport concussion (Cubon et al., 2011; Murugavel et al., 2014). Based on NPLS analyses, these effects are also associated with concurrent reductions in V_{IC}. This suggests that the primary effect of concussion on white matter is increased extra-neurite water volume, at both early injury and RTP. In contrast, the absence of significant V_{ISO} effects indicates that the DTI findings are not primarily driven by variations in free water volume. In addition, based on the absence of significant ODI effects, the changes in compartment water volumes do not appear to systematically alter neurite geometry. Given the significant effects at SYM and RTP relative to CTL, current results also indicate that there is limited change in the microstructural properties of white matter over the course of clinical recovery. Although univariate results showed sparse longitudinal (RTP–SYM) changes, including decreases in FA and increases in AD, RD, and ODI, the lack of longitudinal NPLS results indicate that the effects are spatially heterogeneous, with limited covariation of DTI and NODDI parameters. However, prior longitudinal DTI analyses have found reliable changes in white matter at 6 months post-injury (Henry et al., 2011), hence greater effects may appear over a timespan longer than the typical time to RTP, which was a median of 19 days post-injury in the present study.

The observed effects may be driven by multiple physiological responses to concussion. Early injury is associated with glial-mediated edema, which may be of either intracellular (Marmarou, 2007; Unterberg, Stover, Kress, & Kiening, 2004) or vasogenic (Unterberg et al., 2004) origin, either of which may lead to an increase in extra-neurite water volume. However, the presence of white matter effects at RTP suggest a longer-term neurobiological response that persists for weeks to months post-injury. One candidate mechanism for these findings is neuroinflammation, which has been identified days to months after traumatic insult (Patterson & Holahan, 2012) and has been linked to disruptions in the blood–brain barrier of concussed athletes (Marchi et al., 2013). The neuroinflammatory response is mediated by glial activation, including enlargement of microglia and astrocytes (Streit, Mrak, & Griffin, 2004), which would also serve to increase extra-neurite water volume. The presence of a long-term neuroinflammatory response in sport concussion is supported by prior research, in which peripheral biomarkers of neuroinflammation were seen in athletes years after their last concussion (Di Battista et al., 2016). Although the present findings are similar to more severe TBI, where they have been linked to neurodegeneration (Arfanakis et al., 2002; Inglese et al., 2005; Nakayama et al., 2006; Newcombe et al., 2009), the presence of these effects at early injury and the modest levels of clinical impairment make it unlikely that neurodegeneration is the main cause of the observed effects. Moreover, although reliable group-level effects are observed, the individual subject effects of concussion on DTI and NODDI parameters are variable, with few concussed athletes showing significant abnormalities based on the control 95% CIs shown in Figure 2c, suggesting a subtle and/or heterogeneous neurobiological effect.

Covariate analysis showed longitudinal changes in diffusion parameters, relating to both SCAT symptom severity and time to RTP. This is in contrast to prior DTI research, which found no effects of time to RTP (Churchill, Hutchison, et al., 2017b), although the preceding study employed a univariate regression approach. In the present study, voxel saliences (Figure 3a) were spatially sparse and had small bootstrap ratios compared with group-level results (Figure 2a). Thus, the covariate effects are relatively weak and/or spatially heterogeneous in this cohort and detection likely requires the increased power of combined DTI/NODDI data and multivariate analysis. The NPLS analysis showed that, for individuals with elevated symptoms and prolonged recovery, there were greater longitudinal effects of concussion, including decreasing FA and increasing AD and RD. Interestingly, this was coupled with increasing ODI but without a significant change in V_{IC}. Hence, NODDI may be able to detect microstructural effects that are specifically associated with severity of clinical outcome following a concussion. The change in neurite geometry, in the absence of altered V_{IC}, may reflect long-term neuroplastic response to injury, as seen in more severe TBI (Dancause et al., 2005; Sidaros et al., 2007). Alternatively, there may be a decrease in intracellular water which is heterogeneously mixed into extracellular and isotropic water fractions, leading to apparent inconsistent changes in tissue water. Further research will be required to more fully characterize the relationship between clinical covariates and diffusion imaging measures.

This study has some limitations. First, the NODDI results are based on diffusion shells with differing TR/TE values. Although simulation results included in this study indicate that the renormalization approach can effectively correct for this issue (Supporting Information Appendix S1), future research should also validate the results using fixed TR/TE values. In addition, the current NODDI parameter estimates are based on compartment models developed primarily for normal, healthy adult tissue. For example, the analyses were based on standard values of intrinsic diffusivity (Zhang et al., 2012), but an error in estimated diffusivity can substantially alter apparent V_{IC} (Hutchinson et al., 2017). Thus, the effect of concussion on neurite volume may be confounded by other factors, including changes in

properties of tissue water (e.g., altered viscosity) or changes in myelination status (Grussu et al., 2017). Comparison with controls presumes a similar physiology, which is reasonable given the relatively mild nature of TBI in this cohort, but future research may benefit from more advanced concussion-specific diffusion models. The present findings may also be strengthened by including other advanced diffusion models such as diffusion kurtosis imaging (Jensen, Helpern, Ramani, Lu, & Kaczynski, 2005) to gain further insights into how concussion affects brain tissue, and how different diffusion imaging parameters are inter-related. In this study, a lack of pre-injury baseline imaging also precludes determination of whether the observed DTI and NODDI effects are direct sequelae of injury or were present prior to the concussion. Given the presence of abnormalities at RTP, it is also not clear if the observed differences in white matter are static, or show ongoing change over longer timescales (e.g., months to years). Future research should therefore also examine diffusion imaging parameters over a longer timeline post-injury.

The present study has extended our understanding of the effects of concussion on neural microstructure from early symptomatic injury to RTP, thereby validating standard DTI findings among young, currently active athletes. DTI markers of brain injury are principally associated with reduced intra-neurite volume, at the symptomatic phase of injury and following RTP. Moreover, the longitudinal evolution of DTI parameters is affected by acute symptom severity and time to RTP and mainly associated with greater neurite orientation dispersion. This work demonstrates the importance of using advanced diffusion MRI models including NODDI to better understand how brain tissue is altered during recovery after a concussion.

ACKNOWLEDGMENTS

This work was supported by the Canadian Institutes of Health Research (CIHR) [grant number RN294001-367456]; the Canadian Institute for Military and Veterans Health (CIMVHR) [grant number W7714-145967]; and funding from Siemens Canada Ltd.

ORCID

Nathan W. Churchill https://orcid.org/0000-0001-8481-2505

REFERENCES

Arfanakis, K., Haughton, V. M., Carew, J. D., Rogers, B. P., Dempsey, R. J., & Meyerand, M. E. (2002). Diffusion tensor MR imaging in diffuse axonal injury. *American Journal of Neuroradiology*, *23*, 794–802.

Bazarian, J. J., Zhu, T., Blyth, B., Borrino, A., & Zhong, J. (2012). Subject-specific changes in brain white matter on diffusion tensor imaging after sports-related concussion. *Magnetic Resonance Imaging*, *30*, 171–180.

Bro, R. (1996). Multiway calibration. Multilinear PLS. *Journal of Chemometrics*, *10*, 47–61.

Chang, Y. S., Owen, J. P., Pojman, N. J., Thieu, T., Bukshpun, P., Wakahiro, M. L., … Sherr, E. H. (2015). White matter changes of neurite density and fiber orientation dispersion during human brain maturation. *PLoS One*, *10*, e0123656.

Churchill, N., Spring, R., Abdi, H., Kovacevic, N., McIntosh, A. R., & Strother, S. (2013). The stability of behavioral PLS results in ill-posed neuroimaging problems. In H. Abdi, W. W. Chin, V. Esposito Vinzi, G. Russolillo, & L. Trinchera (Eds.), *New perspectives in partial least squares and related methods* (pp. 171–183). New York, NY: Springer.

Churchill, N. W., Caverzasi, E., Graham, S. J., Hutchison, M. G., & Schweizer, T. A. (2017a). White matter microstructure in athletes with a history of concussion: Comparing diffusion tensor imaging (DTI) and neurite orientation dispersion and density imaging (NODDI). *Human Brain Mapping*, *38*, 4201–4211.

Churchill, N. W., Hutchison, M. G., Richards, D., Leung, G., Graham, S. J., & Schweizer, T. A. (2017b). Neuroimaging of sport concussion: Persistent alterations in brain structure and function at medical clearance. *Scientific Reports*, *7*, 8297.

Cubon, V., Putukian, M., Boyer, C., & Dettwiler, A. (2011). A diffusion tensor imaging study on the white matter skeleton in individuals with sports-related concussion. *Journal of Neurotrauma*, *28*, 189–201.

Dancause, N., Barbay, S., Frost, S. B., Plautz, E. J., Chen, D., Zoubina, E. V., … Nudo, R. J. (2005). Extensive cortical rewiring after brain injury. *Journal of Neuroscience*, *25*, 10167–10179.

Dean, P. J., Sato, J. R., Vieira, G., McNamara, A., & Sterr, A. (2015). Long-term structural changes after mTBI and their relation to post-concussion symptoms. *Brain Injury*, *29*, 1211–1218.

Di Battista, A. P., Rhind, S. G., Richards, D., Churchill, N., Baker, A. J., & Hutchison, M. G. (2016). Altered blood biomarker profiles in athletes with a history of repetitive head impacts. *PLoS One*, *11*, e0159929.

Eierud, C., Craddock, R. C., Fletcher, S., Aulakh, M., King-Casas, B., Kuehl, D., & Laconte, S. M. (2014). Neuroimaging after mild traumatic brain injury: Review and meta-analysis. *NeuroImage: Clinical*, *4*, 283–294.

Grussu, F., Schneider, T., Tur, C., Yates, R. L., Tachrount, M., Ianuş, A., … Alexander, D. C. (2017). Neurite dispersion: A new marker of multiple sclerosis spinal cord pathology? *Annals of Clinical and Translational Neurology*, *4*, 663–679.

Guskiewicz, K., Marshall, S., Bailes, J., McCrea, M., Cantu, R., Randolph, C., & Jordan, B. (2005). Association between recurrent concussion and late-life cognitive impairment in retired professional football players. *Neurosurgery*, *57*, 719–726.

Guskiewicz, K., Register-Mihalik, J., McCrory, P., McCrea, M., Johnston, K., Makdissi, M., & Meeuwisse, W. (2013). Evidence-based approach to revising the SCAT2: Introducing the SCAT3. *British Journal of Sports Medicine*, *47*, 289–293.

Guskiewicz, K., Ross, S., & Marshall, S. (2001). Postural stability and neuropsychological deficits after concussion in collegiate athletes. *Journal of Athletic Training*, *36*, 263.

Henry, L. C., Tremblay, J., Tremblay, S., Lee, A., Brun, C., Lepore, N., … Lassonde, M. (2011). Acute and chronic changes in diffusivity measures after sports concussion. *Journal of Neurotrauma*, *28*, 2049–2059.

Hulkower, M., Poliak, D., Rosenbaum, S., Zimmerman, M., & Lipton, M. L. (2013). A decade of DTI in traumatic brain injury: 10 years and 100 articles later. *American Journal of Neuroradiology*, *34*, 2064–2074.

Hutchinson, E. B., Avram, A. V., Irfanoglu, M. O., Koay, C. G., Barnett, A. S., Komlosh, M. E., … Pierpaoli, C. (2017). Analysis of the effects of noise, DWI sampling, and value of assumed parameters in diffusion MRI models. *Magnetic Resonance in Medicine*, *78*, 1767–1780.

Inglese, M., Makani, S., Johnson, G., Cohen, B. A., Silver, J. A., Gonen, O., & Grossman, R. I. (2005). Diffuse axonal injury in mild traumatic brain injury: A diffusion tensor imaging study. *Journal of Neurosurgery*, *103*, 298–303.

Jensen, J. H., Helpern, J. A., Ramani, A., Lu, H., & Kaczynski, K. (2005). Diffusional kurtosis imaging: The quantification of non-gaussian water diffusion by means of magnetic resonance imaging. *Magnetic Resonance in Medicine*, *53*, 1432–1440.

Krishnan, A., Williams, L., McIntosh, A., & Abdi, H. (2011). Partial least squares (PLS) methods for neuroimaging: A tutorial and review. *NeuroImage*, *56*, 455–475.

Marchi, N., Bazarian, J. J., Puvenna, V., Janigro, M., Ghosh, C., Zhong, J., … Ellis, J. (2013). Consequences of repeated blood-brain barrier disruption in football players. *PLoS One*, *8*, e56805.

Marmarou, A. (2007). A review of progress in understanding the pathophysiology and treatment of brain edema. *Neurosurgical Focus*, *22*, 1–10.

Mayer, A. R., Ling, J. M., Dodd, A. B., Meier, T. B., Hanlon, F. M., & Klimaj, S. D. (2017). A prospective microstructure imaging study in mixed-martial artists using geometric measures and diffusion tensor imaging: Methods and findings. *Brain Imaging and Behavior*, *11*, 698–711.

McAllister, T. W., Ford, J. C., Flashman, L. A., Maerlender, A., Greenwald, R. M., Beckwith, J. G., … Raman, R. (2014). Effect of head

impacts on diffusivity measures in a cohort of collegiate contact sport athletes. *Neurology*, *82*, 63–69.

McCrea, M., Meier, T., Huber, D., Ptito, A., Bigler, E., Debert, C. T., … Wall, R. (2017). Role of advanced neuroimaging, fluid biomarkers and genetic testing in the assessment of sport-related concussion: A systematic review. *The British Journal of Sports Medicine*, *51*, 919–929.

McCrory, P., Meeuwisse, W., Aubry, M., Cantu, B., Dvořák, J., Echemendia, R., & Sills, A. (2013). Consensus statement on concussion in sport: The 4th international conference on concussion in sport held in Zurich. *The British Journal of Sports Medicine*, *47*, 250–258.

McCrory, P., Meeuwisse, W., Dvorak, J., Aubry, M., Bailes, J., Broglio, S., … Castellani, R. J. (2017). Consensus statement on concussion in sport—The 5th international conference on concussion in sport held in Berlin, October 2016. *British Journal of Sports Medicine*, *51*, 838.

Meier, T. B., Bergamino, M., Bellgowan, P. S., Teague, T., Ling, J. M., Jeromin, A., & Mayer, A. R. (2016). Longitudinal assessment of white matter abnormalities following sports-related concussion. *Human Brain Mapping*, *37*, 833–845.

Messé, A., Caplain, S., Pélégrini-Issac, M., Blancho, S., Lévy, R., Aghakhani, N., … Lehéricy, S. (2013). Specific and evolving resting-state network alterations in post-concussion syndrome following mild traumatic brain injury. *PLoS One*, *8*, e65470.

Murugavel, M., Cubon, V., Putukian, M., Echemendia, R., Cabrera, J., Osherson, D., & Dettwiler, A. (2014). A longitudinal diffusion tensor imaging study assessing white matter fiber tracts after sports-related concussion. *Journal of Neurotrauma*, *31*, 1860–1871.

Nakayama, N., Okumura, A., Shinoda, J., Yasokawa, Y., Miwa, K., Yoshimura, S., & Iwama, T. (2006). Evidence for white matter disruption in traumatic brain injury without macroscopic lesions. *Journal of Neurology, Neurosurgery & Psychiatry*, *77*, 850–855.

Newcombe, V., Williams, G., Nortje, J., Bradley, P., Harding, S., Smielewski, P., … Hutchinson, P. (2009). Analysis of acute traumatic axonal injury using diffusion tensor imaging. *British Journal of Neurosurgery*, *21*, 340–348.

Owen, J. P., Chang, Y. S., Pojman, N. J., Bukshpun, P., Wakahiro, M. L., Marco, E. J., … Buckner, R. L. (2014). Aberrant white matter microstructure in children with 16p11.2 deletions. *Journal of Neuroscience*, *34*, 6214–6223.

Patterson, Z. R., & Holahan, M. R. (2012). Understanding the neuroinflammatory response following concussion to develop treatment strategies. *Frontiers in Cellular Neuroscience*, *6*, 58.

Sidaros, A., Engberg, A. W., Sidaros, K., Liptrot, M. G., Herning, M., Petersen, P., … Rostrup, E. (2007). Diffusion tensor imaging during recovery from severe traumatic brain injury and relation to clinical outcome: A longitudinal study. *Brain*, *131*, 559–572.

Smits, M., Houston, G. C., Dippel, D. W., Wielopolski, P. A., Vernooij, M. W., Koudstaal, P. J., … van der Lugt, A. (2011). Microstructural brain injury in post-concussion syndrome after minor head injury. *Neuroradiology*, *53*, 553–563.

Streit, W. J., Mrak, R. E., & Griffin, W. S. T. (2004). Microglia and neuroinflammation: A pathological perspective. *Journal of Neuroinflammation*, *1*, 14.

Unterberg, A., Stover, J., Kress, B., & Kiening, K. (2004). Edema and brain trauma. *Neuroscience*, *129*, 1019–1027.

Wang, Y., Gupta, A., Liu, Z., Zhang, H., Escolar, M. L., Gilmore, J. H., … Gerig, G. (2011). DTI registration in atlas based fiber analysis of infantile Krabbe disease. *NeuroImage*, *55*, 1577–1586.

Zhang, H., Schneider, T., Wheeler-Kingshott, C., & Alexander, D. (2012). NODDI: Practical in vivo neurite orientation dispersion and density imaging of the human brain. *NeuroImage*, *61*, 1000–1016.

SUPPORTING INFORMATION

Additional supporting information may be found online in the Supporting Information section at the end of the article.

How to cite this article: Churchill NW, Caverzasi E, Graham SJ, Hutchison MG, Schweizer TA. White matter during concussion recovery: Comparing diffusion tensor imaging (DTI) and neurite orientation dispersion and density imaging (NODDI). *Hum Brain Mapp*. 2019;40:1908–1918. https://doi.org/10.1002/hbm.24500